

## Multimodality Imaging of Heart Valve Disease

Ronak Rajani<sup>1</sup>, Rajdeep Khattar<sup>2</sup>, Amedeo Chiribiri<sup>3</sup>, Kelly Victor<sup>1</sup>, John Chambers<sup>1</sup>

Department of Cardiology, St. Thomas' Hospital<sup>1</sup>, London; Department of Cardiology, Royal Brompton Hospital<sup>2</sup>, London; Divisions of Imaging Sciences, The Rayne Institute, St. Thomas' Hospital<sup>3</sup>, London – United Kingdom

### Glossary

**VENC** – Velocity Encoding – a specialized technique for encoding flow-velocities on cardiac magnetic resonance imaging.

**SSFP** – Steady-State Free Precession – a gradient echo magnetic resonance imaging pulse sequence in which a steady, residual transverse magnetization is maintained between successive cycles.

### Abstract

Unidentified heart valve disease is associated with a significant morbidity and mortality. It has therefore become important to accurately identify, assess and monitor patients with this condition in order that appropriate and timely intervention can occur. Although echocardiography has emerged as the predominant imaging modality for this purpose, recent advances in cardiac magnetic resonance and cardiac computed tomography indicate that they may have an important contribution to make. The current review describes the assessment of regurgitant and stenotic heart valves by multimodality imaging (echocardiography, cardiac computed tomography and cardiac magnetic resonance) and discusses their relative strengths and weaknesses.

### Introduction

Heart valve disease causes significant morbidity and premature death but also carries a sizeable health economic burden. The population prevalence of moderate or severe valve disease is 2.5% in industrially developed countries<sup>1</sup>, but this rises to 13% at age  $\geq 75$  years. Therefore, as our population ages, clinicians will increasingly need to identify and monitor valve disease. Judging the appropriateness and timing of interventions will become progressively harder in the face of cardiac and extracardiac comorbidities.

### Keywords

Diagnostic Imaging; Heart Valve Diseases; Cardiac Imaging; Techniques/ trends; Magnetic Resonance Imaging; Tomography.

**Mailing address: Ronak Rajani** •

Department of Cardiology, Westminster Bridge Road, St Thomas' Hospital, London, SE1 7EH. United Kingdom.

E-mail: Dr.R.Rajani@gmail.com

Manuscript received October 28, 2013; revised January 7, 2014; accepted January 7, 2014.

**DOI:** 10.5935/abc.20140057

Echocardiography is the cornerstone of assessing heart valve disease. It is affordable, accessible and backed by a strong evidence base (Table 1)<sup>2</sup>. However, cardiac magnetic resonance imaging and cardiac computed tomography (CT) are increasingly useful. This review addresses the roles and limitations of each of these modalities for the assessment of patients with heart valve disease.

### The aortic valve

#### Echocardiography

##### Aortic stenosis

Aortic stenosis (AS) is differentiated from 'sclerosis' by a reduction in valve opening (Figure 1) with a peak transaortic velocity  $> 2.5$  m/s. It is graded using a minimum dataset of the peak velocity, mean pressure gradient and effective orifice area (EOA)<sup>3,4</sup>. (Table 1).

Echocardiography provides information on left ventricular (LV) systolic and diastolic anatomy and function. It also assesses the rest of the heart especially the aorta, the mitral valve and the right heart. Exercise echocardiography may reveal indications for surgery in patients with asymptomatic severe AS: symptoms (Class I), a fall in blood pressure below baseline (Class IIa) or an increase in mean gradient of  $> 20$  mmHg (Class IIb)<sup>5</sup>.

##### Discrepant measures of Aortic Stenosis severity

It is relatively common to find that the velocity and gradient are discrepant with the EOA. The first step should be to review the measurements (Table 2) looking for errors. Transvalvular gradients in the severe range and the EOA in the moderate range may be caused by erroneously low placement of the pulsed sample volume and the diameter of the LV outflow tract (LVOT) may be difficult to measure correctly. This situation can also be a genuine effect of increased flow for example as a result of sepsis, anaemia, or coexistent significant aortic regurgitation (AR).

If the velocity and gradient are moderate but the EOA is severe, the situation has a number of possible explanations. There is evidence that the cut-points for orifice area may not be valid and effective areas between 0.8 and 1.0 cm<sup>2</sup> may sometimes be moderate rather than severe. The shape of the waveform and appearance and mobility of the valve may help to differentiate moderate from severe and it may also help to index EOA to body surface area (BSA).

$$^{\circ}\text{EOA} = \frac{\text{CSA}_{\text{LVOT}} \times \text{VTI}_{\text{LVOT}}}{\text{VTI}_{\text{AV}}}$$

Where: AV: aortic valve; CSA: cross sectional area; EOA: effective orifice area; LVOT: left ventricular outflow tract; VTI: velocity-time integral.

**Table 1 – Severity grading of heart valve disease**

	Mild	Moderate	Severe
<b>Aortic stenosis</b>			
Peak velocity (m/s)	< 3	3-4	> 4
Mean gradient (mmHg)	< 25 (< 30*)	25-40 (30-50*)	> 40 (> 50*)
Valve area (cm <sup>2</sup> )	> 1.5	1-1.5	< 1
Indexed valve area (cm <sup>2</sup> /m <sup>2</sup> )	> 0.85	0.60-0.85	< 0.60
Velocity ratio	> 0.50	0.25-0.5	< 0.25
<b>Aortic regurgitation</b>			
Colour Doppler width (%)	< 25	25-65	> 65%
Regurgitant volume (mls/beat)	< 30	30-59	≥ 60
Vena contracta width	< 3		> 6
Regurgitant fraction (%)	< 30	30-49	≥ 50
Pressure half-time (msec)	> 500*	250-450	< 200*
<b>Mitral stenosis</b>			
Valve area (cm <sup>2</sup> )	> 1.5	1-1.5	< 1
Mean gradient (mmHg)	< 5	5-10	> 10
Pulmonary artery pressure (mmHg)	< 20	30-50	> 50
<b>Mitral regurgitation</b>			
Vena contracta width (mm)	< 3	3-7	> 7
Regurgitant volume (mls/beat)	< 30	30-59	≥ 60 <sup>a</sup> / ≥ 30 <sup>b</sup>
Regurgitant fraction (%)	< 30	30-49	> 50
Regurgitant orifice area (cm <sup>2</sup> )	< 0.2	0.2-0.39	≥ 0.4 <sup>a</sup> / ≥ 0.2 <sup>b</sup>
<b>Tricuspid stenosis</b>			
Valve area (cm <sup>2</sup> )			< 1
<b>Tricuspid regurgitation</b>			
Vena contracta width (mm)			7
Flow reversal - hepatic veins			Present
<b>Pulmonary stenosis</b>			
Peak gradient (mmHg)			> 60
<b>Pulmonary regurgitation</b>			
Pressure half-time (msec)			< 100

*Adapted from: Bonow and cols.<sup>2</sup>.*

*\* European Association of Echocardiography recommendations<sup>13</sup>.*

*Thresholds for primary<sup>a</sup> and secondary<sup>b</sup> mitral regurgitation.*

If the LVOT diameter is thought to be inaccurate, the use of the dimensionless velocity ratio may also give a guide. However it is increasingly recognised that this situation can be caused by low flow.

Traditionally low flow AS was diagnosed by an EOA < 1 cm<sup>2</sup>, mean gradient < 30 to 40 mmHg<sup>6</sup> and LV ejection fraction < 40%. However a thick-walled LV with a small cavity can eject a low stroke volume even with a normal ejection fraction. Low flow may then be recognised with a subaortic velocity integral of < 15 cm, indexed stroke volume 35 mL/m<sup>2</sup> or a calculated flow of < 200 mL/s. If the LV ejection fraction is low or if the EOA is just within the severe range

and the gradient only low moderate, a dobutamine stress echocardiogram should be considered. This confirms severe AS if the mean gradient exceeds 30 to 40 mmHg during any stage of the dobutamine infusion, provided that the EOA remains < 1.2 cm<sup>2</sup><sup>7-9</sup>. It also determines LV contractile reserve shown by an increase in stroke volume, velocity integral or ejection fraction by > 20%.

### The effect of aortic physiology

Hypertension or the resulting decreased aortic compliance adds to the resistance at the aortic valve (AV) to increase the

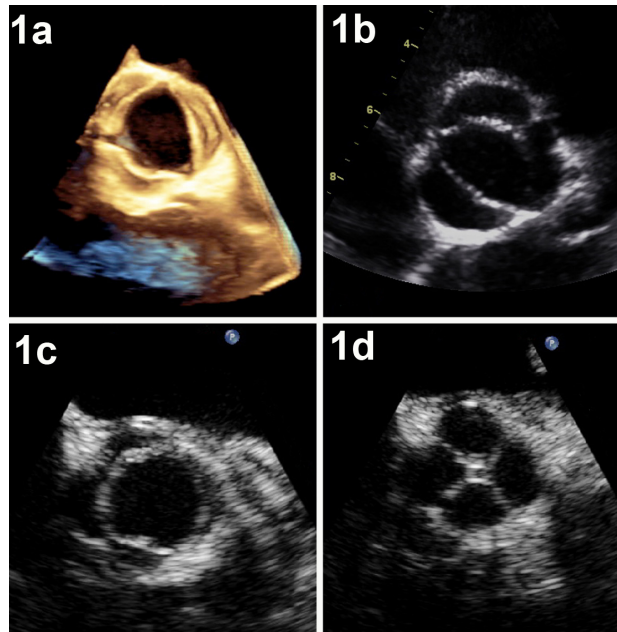


**Figure 1** – Echocardiographic appearances of the aortic valve in short axis. Figure 1A shows the three-dimensional appearance of a tricuspid aortic valve on transoesophageal echocardiography; Figure 1B shows the appearance of a bicuspid aortic valve on transthoracic echocardiography; and Figures 1C and 1D shows the appearances of a quadricuspid aortic valve in systole and diastole.

**Table 2** – Resolving discrepant measurements of aortic stenosis severity

Severe area ( $< 1.0 \text{ cm}^2$ ) Moderate gradient ( $< 30\text{-}40 \text{ mmHg}$ )	Assess valve opening Assess waveform shape (triangular = moderate) Index EOA to BSA (Table 1) If EF $< 40\%$ or VTI $< 15$ consider stress echocardiogram
Severe gradient (V max $> 4\text{ m/s}$ ) Moderate area ( $> 1.0 \text{ cm}^2$ )	Check positioning of sub-aortic pulsed sample is away from the valve Check measurement of LVOT diameter Flow may be increased because of concomitant aortic regurgitation (assess valve opening and waveform shape)

EOA: effective orifice area; BSA: body surface area; EF: ejection fraction; VTI: velocity-time integral; LVOT: left ventricular outflow tract.

total LV outflow impedance. This may result in severe LV systolic or diastolic dysfunction, even if the AS is moderate<sup>10-12</sup>. Blood pressure measurements should ideally be taken at the time of echocardiography to ensure valid comparison between serial studies<sup>13</sup> using a number of indices of aortic and AV combined impedance<sup>14-17</sup>. However, these are not in routine clinical use pending long-term outcome data.

### Aortic Regurgitation

The aetiology is shown on two-dimensional imaging and may be valvar or secondary to aortic dilatation or both<sup>18,19</sup>. Valve diseases include calcific disease, bicuspid AV, infective endocarditis and rheumatic disease. Colour Doppler provides a semi-quantitative assessment (Figure 2). Severe regurgitation is shown by a vena contracta width  $> 6 \text{ mm}$  or the height of the jet  $\geq 65\%$  LVOT diameter<sup>2,20</sup>. The pressure half-time of the continuous wave (CW) Doppler signal is less reliable because

it also depends on LV diastolic pressure, chamber compliance and systemic vascular resistance<sup>21</sup>. Severe AR is also confirmed by the detection of pandiastolic flow reversal in the proximal descending aorta with an end-diastolic velocity typically  $> 20 \text{ cm/s}$ <sup>22</sup> (Figure 2). The regurgitant volume (RVol) and fraction can be calculated by either pulsed wave (PW) Doppler or by the proximal isovelocity surface area method. A RVol of  $\geq 60 \text{ ml}$  and a regurgitant fraction of  $\geq 50\%$  are taken to be indicative of severe AR<sup>2</sup>.

### Evaluation of the left ventricle

With chronic AR, the left ventricle dilates and there is eccentric hypertrophy to ameliorate the ensuing increase in wall stress. Subendocardial fibrosis develops and as the LV ejection falls, LV failure will ultimately supervene, if surgery is not performed. In asymptomatic severe AR, surgery is therefore indicated when the LVEF  $\leq 50\%$

(Class I indication) or with a left ventricular end diastolic dimension (LVEDD) > 70 mm, or left ventricular end systolic diameter (LVESD) > 50 mm (or BSA indexed LVESD > 25 mm/m<sup>2</sup>) (Class IIa). Newer measures of subclinical LV impairment (strain and tissue Doppler imaging) have been proposed but are not in clinical use.

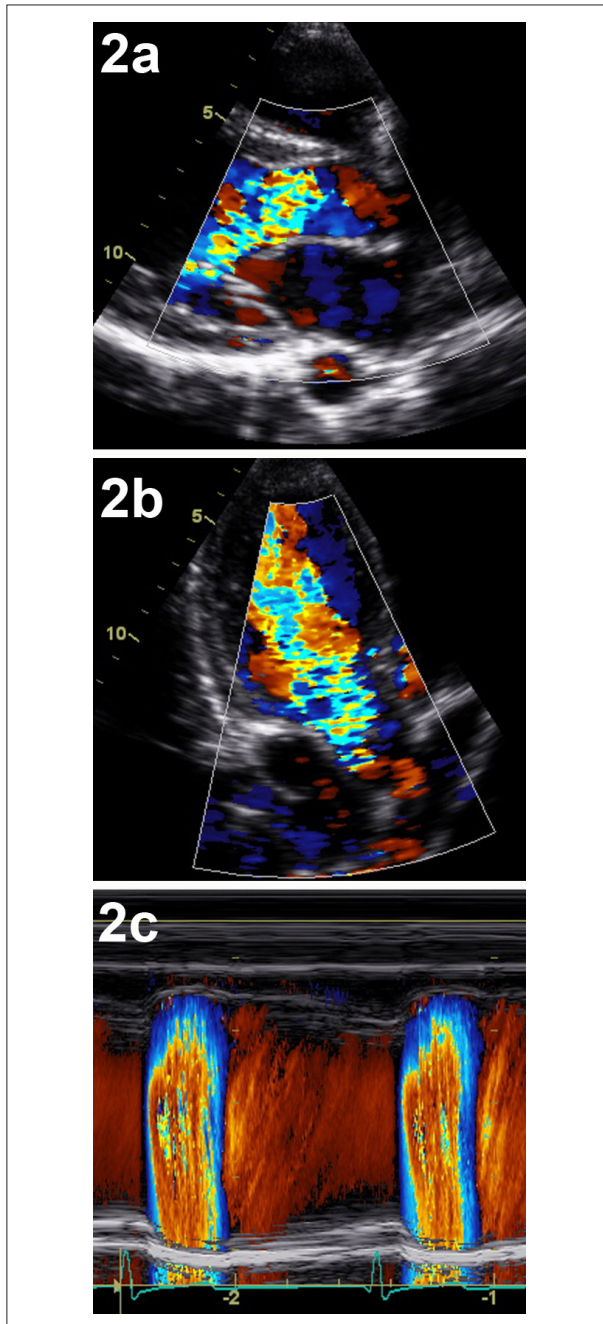


**Figure 2** – Two-dimensional transthoracic appearances of severe aortic regurgitation. Figure 2A shows the aortic regurgitant jet occupying 100% of the left ventricular outflow tract diameter in the parasternal long axis view and Figure 2B, 100% of the left ventricular outflow tract in the apical three chamber view. Figure 2C shows pandiastolic flow reversal in the proximal descending aorta on colour M-Mode.

There is no clear role for stress echocardiography in AR although the evaluation of symptoms may be useful.

### Cardiac Computed Tomography

#### Aortic Stenosis

Coincidental AV calcification on a routine non-contrast enhanced CT scan may alert clinicians to the need for echocardiography (Figure 3)<sup>23-25</sup>. However, CT is not a first line investigation because it cannot provide haemodynamic data and requires ionising radiation and iodinated contrast agents. Imaging of the AV must be performed in both systole and diastole to permit reconstructions at every 5% to 10% of the cardiac cycle. From these, the geometric orifice area can be estimated by planimetry (Figure 3)<sup>26</sup>. CT can also provide LV volume and function, and accurate measurements of the ascending aorta. It can quantify calcium if a ‘porcelain’ aorta is suspected on the echocardiogram or invasive coronary angiogram. CT is essential for evaluating the aortic root before transcatheter AV implantation<sup>27,28</sup>, and can detect pannus and evaluate prosthetic valve function<sup>29</sup>. CT may also be used for the assessment of concomitant coronary disease before AV surgery especially in the presence of AV vegetations (Table 3).

#### Aortic Regurgitation

The role of cardiac CT in the assessment AR is limited. If appropriate phase reconstructions from the cardiac cycle are available from a cardiac CT scan performed for other reasons (e.g. coronary imaging), then it is reasonable to use multiplanar reformatted images to assess the configuration and morphology of the AV and to look for areas of malcoaptation of the valve leaflets. Although malcoaptation on cardiac CT has been shown to have a sensitivity of 95% and specificity of 95% to 100% for the detection of moderate-severe AR, measurements of the AR area by planimetry are less reliable when compared to transthoracic echocardiography (TTE) as a gold standard<sup>30,31</sup>.

### Cardiac magnetic resonance

#### Aortic Stenosis

AS may be detected on cardiovascular magnetic resonance (CMR) by the identification of flow turbulence on bright blood sequences within the LVOT and into the ascending aorta (Table 4 and Figure 4). The valve can be imaged using bright blood sequences. The geometric orifice area, measured by planimetry, correlates well, but systematically underestimates compared with TEE (Figures 5 and 6)<sup>32-35</sup>. The main reasons for this are the complex three-dimensional shape of the stenotic orifice, the leaflet calcification and the associated jet turbulence making an accurate visualization of the true stenotic orifice difficult. CMR has the added benefit of being able to measure flow and velocity across any tubular structure using velocity encoded (VENC) contrast sequences. With optimal plane selection at the aortic root, the peak transaortic velocity can be obtained from which the peak instantaneous gradient can be derived, using the simplified Bernoulli equation ( $4V^2$ ). This technique requires careful mapping of



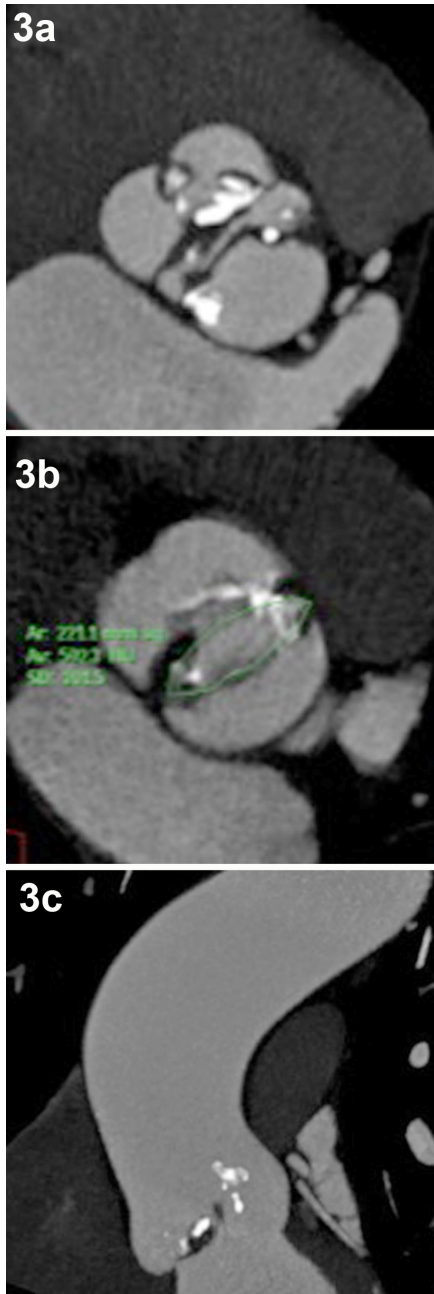


**Figure 3** – Cardiac computed tomography of a bicuspid aortic valve. Figure 3A shows the morphology and distribution of aortic valve calcium in a patient with a bicuspid aortic valve on a multiplanar reformatted image. Figure 3B shows planimetry of the bicuspid aortic valve and Figure 3C shows the ascending aorta anatomy.

the area of interest for each frame of the cardiac cycle and an appropriate selection of maximum velocity to be programmed into the pulse sequence to avoid aliasing. Peak gradients across the AV by VENC correlate well, but slightly underestimate, the peak gradient obtained CW Doppler on TTE<sup>36-38</sup>.

**Table 3** – Cardiac computerized tomography and the assessment of the aortic valve

	Cardiac computerized tomography
<b>Aortic stenosis</b>	Valve morphology
	Aortic valve calcification
	Accurate aortic annulus size
	Aortic dimensions
	Aortic valve planimetry
	TAVI assessment
	Coronary assessment
<b>Aortic regurgitation</b>	Valve morphology
	Leaflet mal-coaptation
	Aortic dimensions
<b>Suspected endocarditis</b>	Coronary assessment
	Aortic root abscesses
	Localised aneurysm formation

TAVI: transcatheter aortic heart valve.

Cardiac magnetic resonance is the gold standard method of measuring LV mass and volume and can also assess systolic and diastolic LV function. It can differentiate sub-valvular and supra-valvular stenosis by inplane velocity mapping. It can assess the whole aorta, which may be important in patients with a bicuspid AV, in whom the echocardiographic window does not permit adequate imaging above the root. New studies suggest that CMR detects myocardial fibrosis using late Gadolinium enhancement, which may portend a worse clinical outcome<sup>39</sup>.

### Aortic Regurgitation

This can be identified by the detection of diastolic backwards flow into the LVOT upon steady-state free precession (SSFP) cine imaging in the three-chamber/LVOT view (Figure 5). An accurate quantification of RVol and fraction can then be obtained using inplane flow imaging which is able to measure both the forward flow and the regurgitant flow across the AV. From this, the regurgitant fraction can be derived [(RVol/forward flow) x 100]. This technique is dependent upon careful tracing around the area of interest of each frame of the cardiac cycle and the selection of the correct plane at which to measure the forward and regurgitant flows (Figure 5)<sup>40</sup>. CMR's excellent reproducibility for AR flow and LV volumes is useful for serial examinations when determining the timing of surgery<sup>41,42</sup>.

## The mitral valve

### Echocardiography

#### Mitral Regurgitation

Mitral Regurgitation (MR) may be primary (organic) or secondary (functional). Primary causes include mitral

**Table 4 – Imaging principles for heart valve disease using cardiac magnetic resonance imaging**

Electrocardiogram gating
Breath hold acquisitions
Balanced steady-state free precession imaging for cine sequencing in multiple imaging planes (two, three and four chamber's views)
Velocity encoded cine phase contrast imaging in plane and through plane for velocity and flow data
Short axis stack for quantification of regurgitant volume and left ventricular systolic volumes and function
Late gadolinium enhancement for the detection of myocardial fibrosis

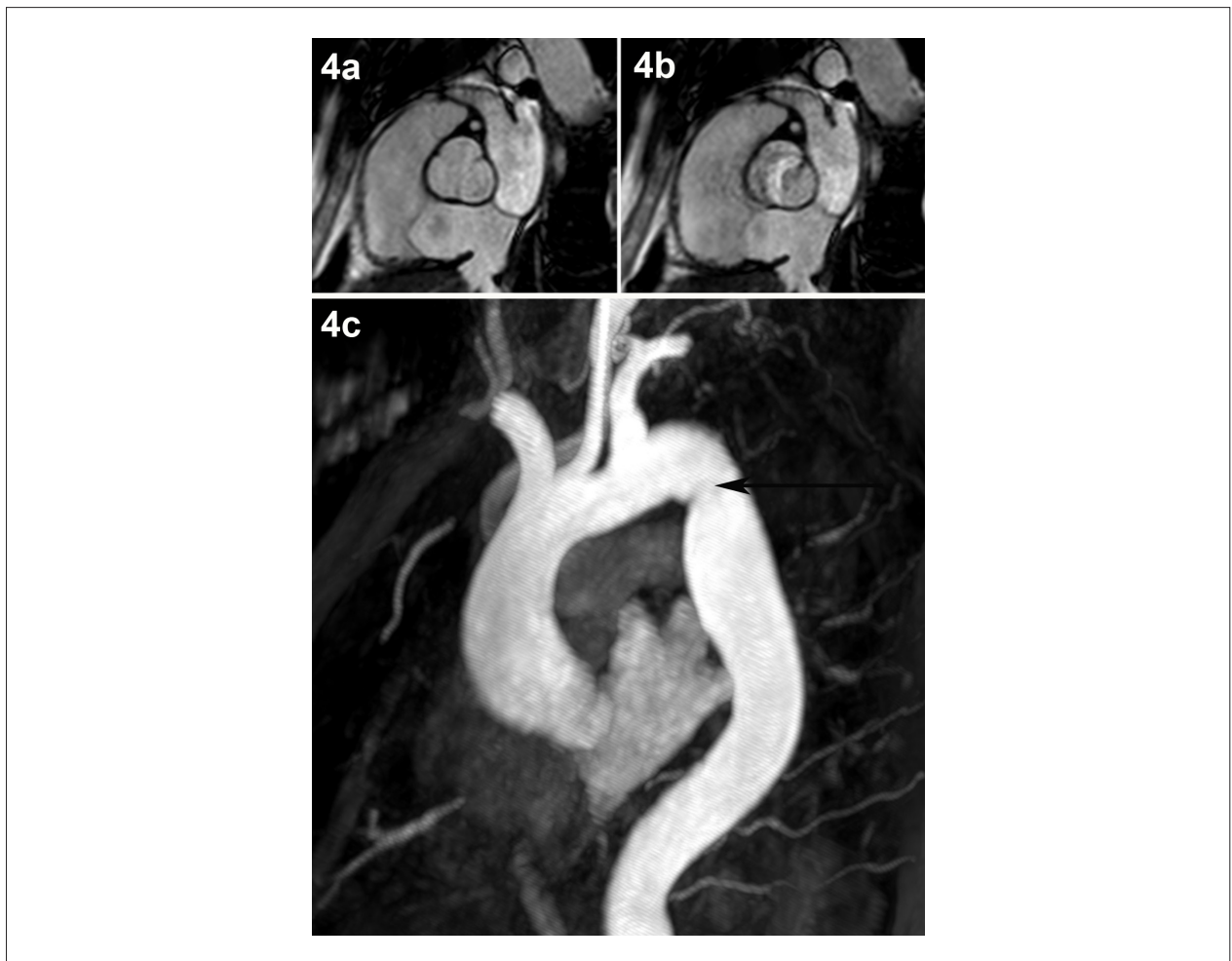


**Figure 4 –** Cardiac magnetic resonance imaging of a bicuspid aortic valve in diastole (A) and systole (B). Turbulence through the aortic valve is seen as white. Figure 4C shows the use of cardiovascular magnetic resonance at also looking at the aortic root in the same patient in who an aortic coarctation was detected (black arrow).

valve prolapse ('degenerative' disease), endocarditis and rheumatic disease. Secondary causes include any causes of LV dysfunction most commonly ischaemic heart disease, hypertension and dilated cardiomyopathy. These can all be detected by echocardiography. Colour Doppler detects MR and quantifies its severity (Figure 6) from the vena contracta width or effective

regurgitant orifice area (EROA), volume (RVol) and regurgitant fraction using the PISA method (Table 1)<sup>2</sup>. Severe MR is likely if the vena contract width is > 7 mm and is supported by a peak transmitral velocity > 1.5 m/s and a mitral VTI: aortic VTI ratio > 1.4<sup>43</sup>. Three-dimensional TTE or transoesophageal echocardiography may provide additional anatomical and quantitative information in

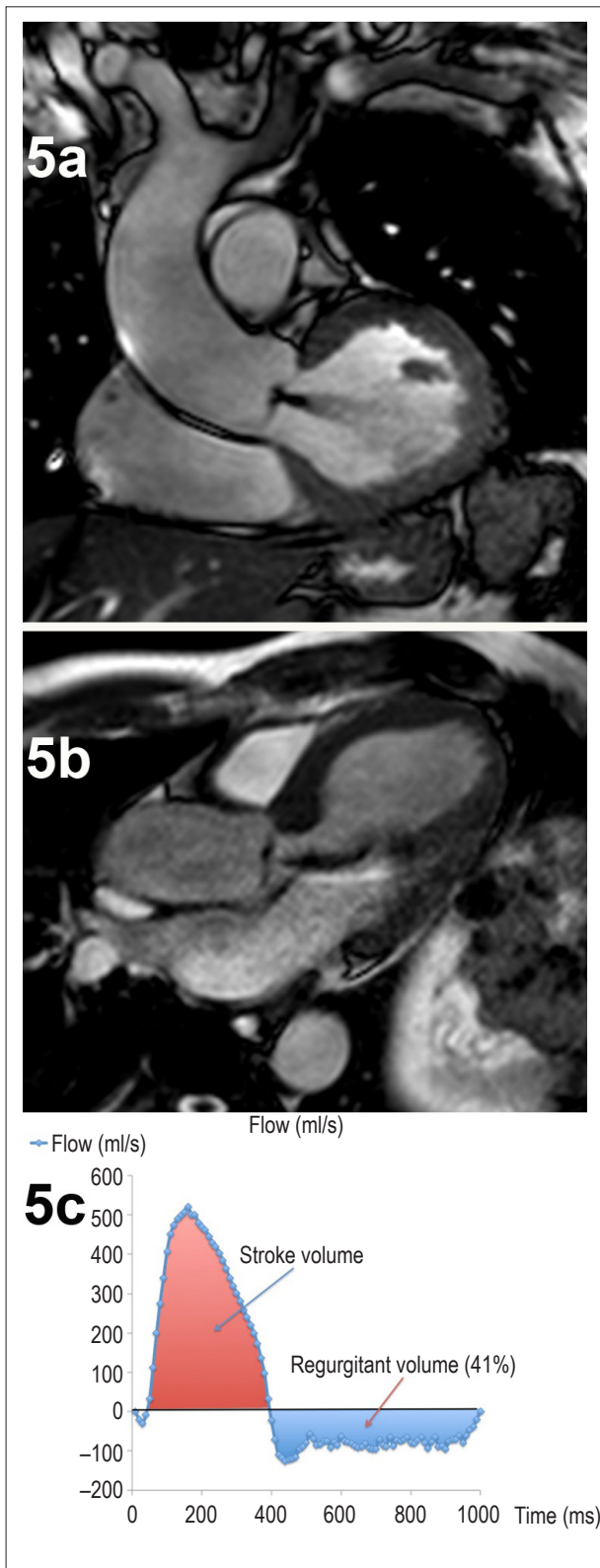


**Figure 5** – Cardiac magnetic resonance imaging of aortic regurgitation using steady-state free precession imaging. The aortic regurgitation is seen as a black jet projecting into the left ventricular cavity in the coronal (5A) and apical five-chamber views (5B). Figure 5C shows a flow/volume curve derived from velocity encoding imaging to calculate the regurgitant volume.

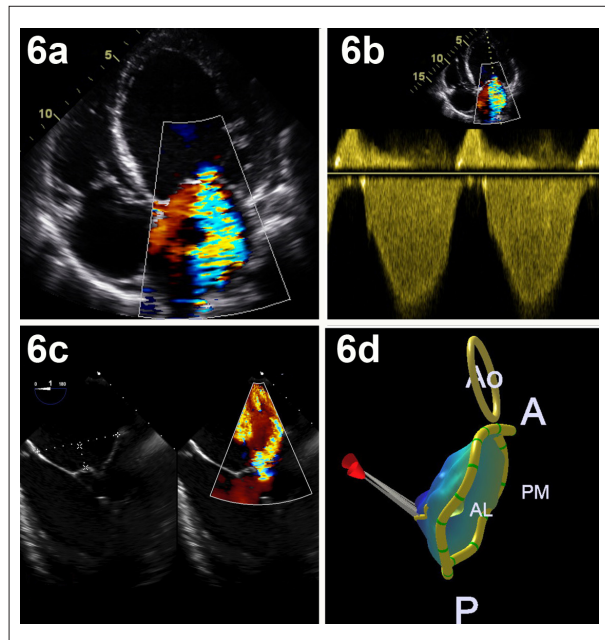


**Figure 6** – Two-dimensional and three-dimensional echocardiographic assessment of mitral regurgitation. Severe mitral regurgitation is seen on colour Doppler imaging in the apical four-chamber view (6A) and on spectral Doppler imaging (6B). Figures 6C and D show the use of three-dimensional transoesophageal echocardiography to model the mitral valve anatomy in an individual with severe function mitral regurgitation.

patients with complex mitral valve lesions (Figure 6). Exercise echocardiography may be useful in patients with discordant symptoms to provide information on changes in MR, LV systolic function and pulmonary artery pressure. An exercise-induced increase in pulmonary artery systolic pressure to  $> 60$  mmHg is a criterion for surgery if repair is feasible. In functional MR caused by ischaemic disease, an exercise-induced increase in EROA  $\geq 13$  mm<sup>2</sup> is associated with a much worse prognosis in those with ischaemic MR.

In asymptomatic patients with severe primary MR surgery is indicated when: the LVEF  $\leq 60\%$  (Class I)<sup>2,5</sup>, or LVESD  $\geq 45$  mm (Class I)<sup>5</sup>, or even  $\geq 40$  mm (Class I)<sup>2</sup> provided the valve is repairable. For patients with secondary MR undergoing coronary artery bypass grafting mitral repair usually with a small annuloplasty ring is recommended if there is moderate or severe regurgitation. However, if surgery is being considered for breathlessness as a result of the MR rather than for ischaemic heart disease, the recommended indications are<sup>5</sup>: (1) if the LVEF is  $< 30\%$  and there is both evidence of significant viability and the possibility of revascularisation or (2) if there is no viability provided the LVEF is  $> 30\%$ , full medical treatment including cardiac resynchronization therapy has been ineffective and there is no significant comorbidity.

### Mitral stenosis

Rheumatic heart disease results in a typical appearance on two-dimensional echocardiography. The leaflet tips are

thickened and commissural fusion results in diastolic bowing of the leaflets in a hockey-stick shaped deformity. The chordae tendinae are also thickened and become matted together. Planimetry of the mitral valve orifice area should be performed using the parasternal short axis on a zoomed mid-diastolic frame<sup>13</sup>. Three-dimensional transthoracic or transoesophageal echocardiography may be useful to select the correct plane for planimetry. A CW Doppler recording across the mitral valve enables the measurement of the mean transmitral gradient and the pressure half-time. The pulmonary artery systolic pressure is estimated using the tricuspid regurgitation (TR) peak velocity ( $4 \times \text{TR V max}$ ) added to an estimated of right atrial mean pressure provided by the size and response of the IVC to a sniff. From the pressure half-time, an estimation of valve area can be made<sup>b 44</sup>.

The grade of mitral stenosis (MS) can then be estimated (Table 1).

Valve EOA can be estimated using the continuity equation or proximal isovelocity surface area method. Exercise echocardiography is indicated in patients with severe symptoms despite apparently only moderate MS. Exercise-induced increases in mean gradient to  $\geq 15$  mmHg or pulmonary artery systolic pressures to  $\geq 60$  mmHg are indications for intervention provided that balloon mitral valvuloplasty is feasible<sup>2</sup>. This is possible in the absence of bicommissural or severe single commissural calcification, severe chordal involvement, calcification and immobility of the valve, more than mild MR, left atrial thrombus and the requirement for intervention for severe involvement of other valves or the coronary arteries<sup>45</sup>.

## Cardiac Computed Tomography

### Mitral Regurgitation

The EROA can be measured by planimetry and this has been shown to correlate well with TEE<sup>46</sup>. Additional information available from cardiac CT includes mitral annulus size, mitral valve leaflet length and calcification, chordae tendinae thickening, left atrial size and the detection of pulmonary oedema. Although cardiac CT with cine imaging can reliably detect and localise segmental leaflet prolapse, this is not routinely performed.

### Mitral stenosis

Cardiac CT is particularly suited to the detection of mitral valve leaflet, commissural and annulus calcification. For an evaluation of the valve components, a reconstruction at 65% of the R-R interval for the open mitral valve and a reconstruction at 5% of the R-R interval are recommended for the closed mitral valve. The geometric orifice area is measured by direct planimetry and has been shown to correlate well with TEE ( $R = 0.88$ ;  $p < 0.001$ )<sup>47</sup>. Additional information obtainable is left atrial size, left atrial appendage thrombus, right ventricular (RV) hypertrophy and radiographic evidence of pulmonary oedema and pulmonary hypertension.

<sup>b</sup>  $MVA = \frac{220}{PH_{\text{Half-time}}}$

Where: MVA: mitral valve area; PH<sub>Half-time</sub>: pressure half-time.

## Cardiac magnetic resonance imaging

### Mitral Regurgitation

MR is initially seen as a net loss of signal across the mitral valve representing flow turbulence on SSFP and gradient echo sequences. For a complete anatomical assessment of the mitral valve bright blood cine sequences should be acquired in the two, three and four chamber planes, along with a full LV short-axis stack. Following this, a basal slice from the short axis stack should be selected where the mitral valve is seen. Oblique slices may then be taken perpendicular to the line of coaptation working down from the A1-P1 juncture inferiorly down to the A3-P3 juncture every 5 mm with no inter-slice gap<sup>48</sup>. This system permits the accurate localisation of regurgitant jets and helps to localise dysfunctional mitral valve leaflet scallops. The RVol can be estimated using the LV stroke volume and forward flow within the aorta at the level of the sinus of valsalva using VENC contrast mapping. The regurgitant fraction is then calculated as the  $[(\text{RVol}/\text{LV stroke volume}) \times 100]$ <sup>49,50</sup>.

### Mitral stenosis

Cardiac magnetic resonance imaging is not used routinely for the assessment of mitral stenosis. Mitral inflow turbulence may be seen on SSFP in-plane imaging and the mitral valve area may be measured using carefully placed through-plane SSFP imaging. Although this technique has been shown to correlate well with echo derived areas<sup>51,52</sup> it is often limited by the presence of atrial fibrillation and problems with electrocardiogram gating.

## The tricuspid valve

### Echocardiography

Causes of primary (organic) tricuspid valve disease include rheumatic disease, endocarditis, prolapse and carcinoid. Secondary (functional) TR is caused by abnormalities of the RV either as a result of infarction, volume or pressure overload. Colour Doppler imaging is the mainstay for quantification with severe TR shown by a vena contracta width  $\geq 7$  mm. Although a vena contracta width  $< 6$  mm is suggestive of less than moderate regurgitation, there are no well validated cut-offs for differentiating mild from moderate TR<sup>53</sup>. Additional markers of severe TR are a pulsed Doppler peak E velocity  $\geq 1$  m/s, a dense CW signal with a fast upstroke (Figure 7) and prominent flow reversal in the hepatic veins<sup>54</sup>. In severe compensated TR, the RV may be normal in size but hyperdynamic. With time, the RV dilates progressively and may become hypodynamic as shown by a tricuspid annulus excursion  $< 15$  mm or a systolic maximum tissue Doppler velocity at the base of the RV free wall of  $< 11$  cm/s<sup>55</sup>.

In severe tricuspid stenosis (TS), the leaflets will be restricted although there may be relatively little thickening compared with left-sided rheumatic disease. Severe stenosis



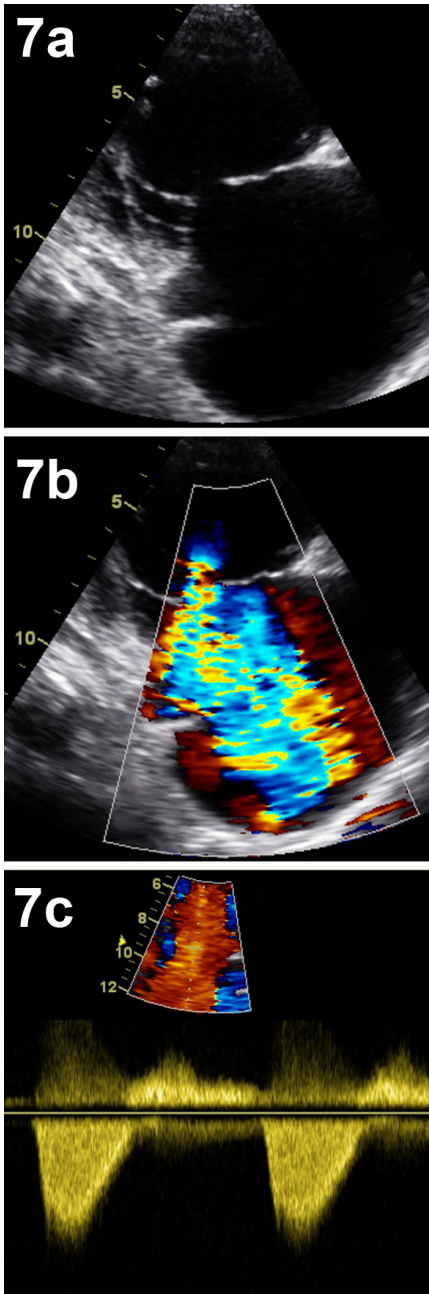


**Figure 7** – Two-dimensional transthoracic echocardiographic appearances of severe tricuspid regurgitation. In the parasternal tricuspid inflow view, there is mal-coaptation of the anterior and posterior tricuspid valve leaflets (7A) that gives rise to a severe jet of regurgitation seen on colour Doppler imaging 7B. Figure 7C shows the continuous wave Doppler appearance of severe tricuspid regurgitation (dagger shape).

is shown by a mean gradient  $\geq 5$  mmHg and pressure half-time  $\geq 190$  ms on CW Doppler and a valve area  $\leq 1$  cm<sup>2</sup> by the continuity equation. Other surrogate measures of significant TS include a dilated right atrium and inferior vena cava reflecting elevated right atrial pressures.

### Cardiac Computed Tomography

Cardiac CT is of limited use in tricuspid valve disease. It can show secondary effects such as right atrial and ventricular dilatation and reflux of contrast into the hepatic veins. Occasionally cardiac CT can identify primary lung causes for TR induced by pulmonary hypertension such as pulmonary fibrosis or pulmonary embolic disease.

### Cardiac magnetic resonance imaging

Significant tricuspid valve disease can be identified by turbulent flow across the tricuspid valve with in-plane SSFP imaging. As with MR, TR can be quantified by measuring RVol and regurgitant fraction from the forward stroke volume in the main pulmonary artery and the measured RV stroke volume on SSFP imaging.

### The pulmonary valve

#### Echocardiography

Two-dimensional imaging may provide clues as to the aetiology of pulmonary valve dysfunction e.g. congenital, endocarditis, carcinoid syndrome. Coexistent congenital anomalies e.g. atrial septal defect (ASD) should be sought since isolated congenital pulmonary valve disease is uncommon. Severe pulmonary valve regurgitation (PR) is shown by a wide jet on colour Doppler (Figure 8) originating in the distal main pulmonary artery or branches, a pressure half-time  $< 100$  ms on CW (Figure 8) and a dilated hyperdynamic RV. For pulmonary stenosis (PS), the primary means for detecting stenosis is the visualisation of calcified leaflets or reduced leaflet excursion on two-dimensional imaging. A peak trans-pulmonary gradient on CW Doppler of  $> 60$  mmHg is taken to usually represent severe PS<sup>2</sup>.

#### Cardiac Computed Tomography

Cardiac CT may be useful in defining complex congenital heart anatomy and for detecting secondary effects of pulmonary valve disease. Dilatation of the pulmonary valve annulus, pulmonary artery dilatation and RV dilatation may be seen with PR, and dilatation of the main pulmonary artery and left and right pulmonary arteries, RV hypertrophy, right atrial enlargement and bowing of the interatrial septum to the left with PS.

#### Cardiac magnetic resonance imaging

Cardiac MR is considered to be the gold standard for the assessment of PR. With visualisation of PR using cine SSFP imaging and the ability to accurately measure RVol and regurgitant fractions with flow imaging, it has now become the technique of choice for the serial evaluation of patients with congenital heart disease, in which progressive RV dilatation and RV dysfunction is important for the timing of pulmonary valve intervention. In patients with PS, turbulent flow can be seen across the pulmonary valve with SSFP cine imaging. Although planimetry of the pulmonary valve is of limited use, CMR is able to provide accurate peak velocity data across the pulmonary valve.

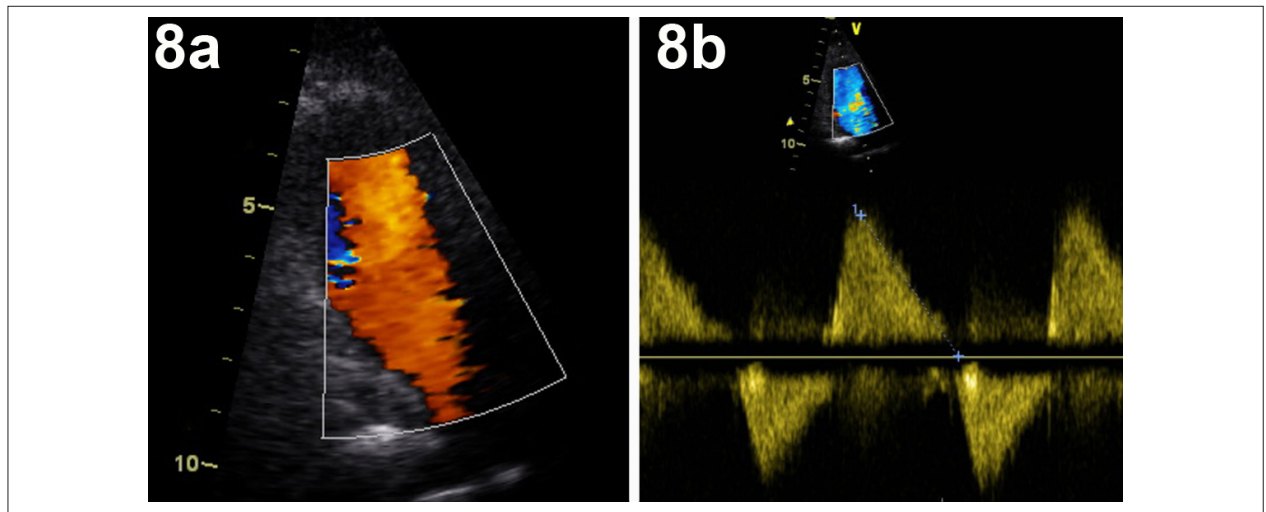


**Figure 8** – Bidimensional transthoracic echocardiographic appearances of severe pulmonary regurgitation. In diastole, the colour Doppler jet is seen to occupy the entirety of the right ventricular outflow tract (8A). On continuous wave Doppler imaging, the pressure half-time is  $< 100\text{ ms}$  in keeping with severe regurgitation (8B).

## Conclusions

Echocardiography is the mainstay for the assessment of patients with valve disease. Where image quality is poor, cardiac magnetic resonance imaging and cardiac computed tomography can both image all valves and provide geometric orifice areas. The ascending aorta is often suboptimally imaged on echocardiography and cardiac magnetic resonance imaging or cardiac computed tomography are commonly needed to fill this deficiency. Both cardiac magnetic resonance imaging and cardiac computed tomography are useful for the assessment of complex anatomy in patients with congenital heart disease. Computed tomography may be used for evaluating coronary disease often before valve surgery. However, it is not indicated for routine valve disease assessment owing to its inability to provide haemodynamic information and its inherent need for iodinated contrast agents and ionising radiation. Cardiac magnetic resonance imaging is valuable for its ability to provide haemodynamic data and also accurate reproducible measurements of ventricular volumes, mass and function. It is considered to be the technique of choice for the assessment of pulmonary valve disease and for detecting myocardial scar.

## References

1. Nkomo VT, Gardin JM, Skelton TN, Gottdiener JS, Scott CG, Enriquez-Sarano M. Burden of valvular heart diseases: a population-based study. *Lancet*. 2006;368(9540):1005-11.
2. Bonow RO, Carabello BA, Chatterjee K, de Leon AC Jr, Faxon DP, Freed MD, et al; American College of Cardiology/American Heart Association Task Force on Practice Guidelines. 2008 focused update incorporated into the ACC/AHA 2006 guidelines for the management of patients with valvular heart disease: a report of the American College of Cardiology/American

## Author contributions

Conception and design of the research: Rajani R, Khattar R, Chiribiri A, Victor K, Chambers J; Acquisition of data: Victor K, Chambers J; Analysis and interpretation of the data: Victor K, Chambers J; Writing of the manuscript: Rajani R; Khattar R, Chiribiri A; Victor K; Critical revision of the manuscript for intellectual content: Rajani R, Khattar R, Chiribiri A, Victor K, Chambers J; Supervision/ as the major investigator: Rajani R, Victor K, Chambers J.

## Potential Conflict of Interest

No potential conflict of interest relevant to this article was reported.

## Sources of Funding

There were no external funding sources for this study.

## Study Association

This study is not associated with any thesis or dissertation work.

Heart Association Task Force on Practice Guidelines (Writing Committee to revise the 1998 guidelines for the management of patients with valvular heart disease). Endorsed by the Society of Cardiovascular Anesthesiologists, Society for Cardiovascular Angiography and Interventions, and Society of Thoracic Surgeons. *J Am Coll Cardiol*. 2008;52(13):e1-142.

3. Otto CM, Pearlman AS, Comess KA, Reamer RP, Janko CL, Huntsman LL. Determination of the stenotic aortic valve area in adults using Doppler echocardiography. *J Am Coll Cardiol*. 1986;7(3):509-17.

4. Zoghbi WA, Farmer KL, Soto JG, Nelson JG, Quinones MA. Accurate noninvasive quantification of stenotic aortic valve area by Doppler echocardiography. *Circulation*. 1986;73(3):452-9.
5. Vahanian A, Alfieri O, Andreotti F, Antunes MJ, Barón-Esquivias G, Baumgartner H, et al; Joint Task Force on the Management of Valvular Heart Disease of the European Society of Cardiology (ESC); European Association for Cardio-Thoracic Surgery (EACTS). Guidelines on the management of valvular heart disease (version 2012): The Joint Task Force on the Management of Valvular Heart Disease of the European Society of Cardiology (ESC) and the European Association for Cardio-Thoracic Surgery (EACTS). *Eur Heart J*. 2012;33(19):2451-96.
6. Chambers J. Low "gradient", low flow aortic stenosis. *Heart*. 2006;92(4):554-8.
7. Monin JL, Quere JP, Monchi M, Petit H, Baleynaud S, Chauvel C, et al. Low-gradient aortic stenosis: operative risk stratification and predictors for long-term outcome: a multicenter study using dobutamine stress hemodynamics. *Circulation*. 2003;108(3):319-24.
8. Nishimura RA, Grantham JA, Connolly HM, Schaff HV, Higano ST, Holmes DR Jr. Low-output, low-gradient aortic stenosis in patients with depressed left ventricular systolic function: the clinical utility of the dobutamine challenge in the catheterization laboratory. *Circulation*. 2002;106(7):809-13.
9. Takeda S, Rimington H, Chambers J. The relation between transaortic pressure difference and flow during dobutamine stress echocardiography in patients with aortic stenosis. *Heart*. 1999;82(1):11-4.
10. Aronow WS, Schwartz KS, Koenigsberg M. Correlation of serum lipids, calcium and phosphorus, diabetes mellitus, aortic valve stenosis and history of systemic hypertension with presence or absence of mitral anular calcium in persons older than 62 years in a long-term health care facility. *Am J Cardiol*. 1987;59(4):381-2.
11. Antonini-Canterin F, Huang G, Cervasato E, et al. Symptomatic aortic stenosis: does systemic hypertension play an additional role? *Hypertension*. 2003;41(6):1268-72.
12. Kadem L, Dumesnil JG, Rieu R, Durand LG, Garcia D, Pibarot P. Impact of systemic hypertension on the assessment of aortic stenosis. *Heart*. 2005;91(3):354-61.
13. Baumgartner H, Hung J, Bermejo J, Chambers JB, Evangelista A, Griffin BP, et al. Echocardiographic assessment of valve stenosis: EAE/ASE recommendations for clinical practice. *Eur J Echocardiogr*. 2009;10(1):1-25. Erratum in: *Eur J Echocardiogr*. 2009;10(3):479.
14. Garcia D, Pibarot P, Dumesnil JG, Sakr F, Durand LG. Assessment of aortic valve stenosis severity: a new index based on the energy loss concept. *Circulation*. 2000;101(7):765-71.
15. Briand M, Dumesnil JG, Kadem L, Tongue AG, Rieu R, Garcia D, et al. Reduced systemic arterial compliance impacts significantly on left ventricular afterload and function in aortic stenosis: implications for diagnosis and treatment. *J Am Coll Cardiol*. 2005;46(2):291-8.
16. Lancellotti P, Donal E, Magne J, Moonen M, O'Connor K, Daubert JC, et al. Risk stratification in asymptomatic moderate to severe aortic stenosis: the importance of the valvular, arterial and ventricular interplay. *Heart*. 2010;96(17):1364-71.
17. Hachicha Z, Dumesnil JG, Bogaty P, Pibarot P. Paradoxical low-flow, low-gradient severe aortic stenosis despite preserved ejection fraction is associated with higher afterload and reduced survival. *Circulation*. 2007;115(22):2856-64.
18. Wan CK, Suri RM, Li Z, Orszulak TA, Daly RC, Schaff HV, et al. Management of moderate functional mitral regurgitation at the time of aortic valve replacement: is concomitant mitral valve repair necessary? *J Thorac Cardiovasc Surg*. 2009;137(3):635-40.
19. Unger P, Dedobbeleer C, Van Camp G, Plein D, Cosyns B, Lancellotti P. Mitral regurgitation in patients with aortic stenosis undergoing valve replacement. *Heart*. 2010;96(1):9-14.
20. Lancellotti P, Tribouilloy C, Hagendorff A, Moura L, Popescu BA, Agricola E, et al; European Association of Echocardiography. European Association of Echocardiography recommendations for the assessment of valvular regurgitation. Part 1: aortic and pulmonary regurgitation (native valve disease). *Eur J Echocardiogr*. 2010;11(3):223-44.
21. Griffin BP, Flachskampf FA, Siu S, Weyman AE, Thomas JD. The effects of regurgitant orifice size, chamber compliance, and systemic vascular resistance on aortic regurgitant velocity slope and pressure half-time. *Am Heart J*. 1991;122(4 Pt 1):1049-56.
22. Tribouilloy C, Avinee P, Shen WF, Rey JL, Slama M, Lesbre JP. End diastolic flow velocity just beneath the aortic isthmus assessed by pulsed Doppler echocardiography: a new predictor of the aortic regurgitant fraction. *Br Heart J*. 1991;65(1):37-40.
23. Messika-Zeitoun D, Aubry MC, Detaint D, Bielak LF, Peyser PA, Sheedy PF, et al. Evaluation and clinical implications of aortic valve calcification measured by electron-beam computed tomography. *Circulation*. 2004;110(3):356-62.
24. Cowell SJ, Newby DE, Burton J, White A, Northridge DB, Boon NA, et al. Aortic valve calcification on computed tomography predicts the severity of aortic stenosis. *Clin Radiol*. 2003;58(9):712-6.
25. Koos R, Kuhl HP, Muhlenbruch G, Wildberger JE, Gunther RW, Mahnen AH. Prevalence and clinical importance of aortic valve calcification detected incidentally on CT scans: comparison with echocardiography. *Radiology*. 2006;241(1):76-82.
26. Shah RG, Novaro GM, Blandon RJ, Whiteman MS, Asher CR, Kirsch J. Aortic valve area: meta-analysis of diagnostic performance of multi-detector computed tomography for aortic valve area measurements as compared to transthoracic echocardiography. *Int J Cardiovasc Imaging*. 2009;25(6):601-9.
27. Willson AB, Webb JG, Labounty TM, Achenbach S, Moss R, Wheeler M, et al. 3-dimensional aortic annular assessment by multidetector computed tomography predicts moderate or severe paravalvular regurgitation after transcatheter aortic valve replacement: a multicenter retrospective analysis. *J Am Coll Cardiol*. 2012;59(14):1287-94.
28. Jilaihawi H, Kashif M, Fontana G, Furugen A, Shiota T, Friede G, et al. Cross-sectional computed tomographic assessment improves accuracy of aortic annular sizing for transcatheter aortic valve replacement and reduces the incidence of paravalvular aortic regurgitation. *J Am Coll Cardiol*. 2012;59(14):1275-86.
29. Konen E, Goitein O, Feinberg MS, Eshet Y, Raanani E, Rimon U, et al. The role of ECG-gated MDCT in the evaluation of aortic and mitral mechanical valves: initial experience. *AJR Am J Roentgenol*. 2008;191(1):26-31.
30. Feuchtner GM, Dichtl W, Schachner T, Müller S, Mallouhi A, Friedrich GJ, et al. Diagnostic performance of MDCT for detecting aortic valve regurgitation. *AJR Am J Roentgenol*. 2006;186(6):1676-81.
31. Feuchtner GM, Dichtl W, Müller S, Müller S, Jodocy D, Schachner T, et al. 64-MDCT for diagnosis of aortic regurgitation in patients referred to CT coronary angiography. *AJR Am J Roentgenol*. 2008;191(1):W1-7.
32. Debl K, Djavidani B, Seitz J, Nitz W, Schmid FX, Muters F, et al. Planimetry of aortic valve area in aortic stenosis by magnetic resonance imaging. *Invest Radiol*. 2005;40(10):631-6.
33. John AS, Dill T, Brandt RR, Rau M, Ricken W, Bachmann G, et al. Magnetic resonance to assess the aortic valve area in aortic stenosis: how does it compare to current diagnostic standards? *J Am Coll Cardiol*. 2003;42(3):519-26.
34. Kupfahl C, Honold M, Meinhardt G, Vogelsberg H, Wagner A, Mahrholdt H, et al. Evaluation of aortic stenosis by cardiovascular magnetic resonance imaging: comparison with established routine clinical techniques. *Heart*. 2004;90(8):893-901.
35. Reant P, Lederlin M, Lafitte S, Serri K, Montaudon M, Corneloup O, et al. Absolute assessment of aortic valve stenosis by planimetry using cardiovascular magnetic resonance imaging: comparison with

- transesophageal echocardiography, transthoracic echocardiography, and cardiac catheterisation. *Eur J Radiol.* 2006;59(2):276-83.
36. Kilner PJ, Manzara CC, Mohiaddin RH, Pennell DJ, Sutton MG, Firmin DN, et al. Magnetic resonance jet velocity mapping in mitral and aortic valve stenosis. *Circulation.* 1993;87(4):1239-48.
  37. Eichenberger AC, Jenni R, von Schulthess GK. Aortic valve pressure gradients in patients with aortic valve stenosis: quantification with velocity-encoded cine MR imaging. *AJR Am J Roentgenol.* 1993;160(5):971-7.
  38. Caruthers SD, Lin SJ, Brown P, Watkins MP, Williams TA, Lehr KA, et al. Practical value of cardiac magnetic resonance imaging for clinical quantification of aortic valve stenosis: comparison with echocardiography. *Circulation.* 2003;108(18):2236-43.
  39. Dweck MR, Joshi S, Murigu T, Alpendurada F, Jabbour A, Melina G, et al. Midwall fibrosis is an independent predictor of mortality in patients with aortic stenosis. *J Am Coll Cardiol.* 2011;58(12):1271-9.
  40. Myerson SG. Heart valve disease: investigation by cardiovascular magnetic resonance. *J Cardiovasc Magn Reson.* 2012;14:7.
  41. Aurigemma G, Reichek N, Schiebler M, Axel L. Evaluation of aortic regurgitation by cardiac cine magnetic resonance imaging: planar analysis and comparison to Doppler echocardiography. *Cardiology.* 1991;78(4):340-7.
  42. Honda N, Machida K, Hashimoto M, Mamiya T, Takahashi T, Kamano T, et al. Aortic regurgitation: quantitation with MR imaging velocity mapping. *Radiology.* 1993;186(1):189-94.
  43. Tribouilloy C, Shen WF, Rey JL, Adam MC, Lesbre JP. Mitral to aortic velocity-time integral ratio: a non-geometric pulsed-Doppler regurgitant index in isolated pure mitral regurgitation. *Eur Heart J.* 1994;15(10):1335-9.
  44. Thomas JD, Weyman AE. Doppler mitral pressure half-time: a clinical tool in search of theoretical justification. *J Am Coll Cardiol.* 1987;10(4):923-9.
  45. Wilkins GT, Weyman AE, Abascal VM, Block PC, Palacios IF. Percutaneous balloon dilatation of the mitral valve: an analysis of echocardiographic variables related to outcome and the mechanism of dilatation. *Br Heart J.* 1988;60(4):299-308.
  46. Alkadhi H, Wildermuth S, Bettex DA, Plass A, Baumert B, Leschka S, et al. Mitral regurgitation: quantification with 16-detector row CT--initial experience. *Radiology.* 2006;238(2):454-63.
  47. Messika-Zeitoun D, Serfaty JM, Laissy JP, Berhili M, Brochet E, Jung B, et al. Assessment of the mitral valve area in patients with mitral stenosis by multislice computed tomography. *J Am Coll Cardiol.* 2006;48(2):411-3.
  48. Chan KM, Wage R, Symmonds K, Rahman-Haley S, Mohiaddin RH, Firmin DN, et al. Towards comprehensive assessment of mitral regurgitation using cardiovascular magnetic resonance. *J Cardiovasc Magn Reson.* 2008;10:61.
  49. Kon MW, Myerson SG, Moat NE, Pennell DJ. Quantification of regurgitant fraction in mitral regurgitation by cardiovascular magnetic resonance: comparison of techniques. *J Heart Valve Dis.* 2004;13(4):600-7.
  50. Kizilbash AM, Hundley WC, Willett DL, Franco F, Peshock RM, Grayburn PA. Comparison of quantitative Doppler with magnetic resonance imaging for assessment of the severity of mitral regurgitation. *Am J Cardiol.* 1998;81(6):792-5.
  51. Djavidani B, Debl K, Lenhart M, Seitz J, Paetzel C, Schmid FX, et al. Planimetry of mitral valve stenosis by magnetic resonance imaging. *J Am Coll Cardiol.* 2005;45(12):2048-53.
  52. Djavidani B, Debl K, Buchner S, Lipke C, Nitz W, Feuerbach S, et al. MRI planimetry for diagnosis and follow-up of valve area in mitral stenosis treated with valvuloplasty. *Rofo.* 2006;178(8):781-6.
  53. Lancellotti P, Moura L, Pierard LA, Agricola E, Popescu BA, Tribouilloy C, et al. European Association of Echocardiography recommendations for the assessment of valvular regurgitation. Part 2: mitral and tricuspid regurgitation (native valve disease). *Eur J Echocardiogr.* 2010;11(4):307-32.
  54. Gonzalez-Vilchez F, Zarauza J, Vazquez de Prada JA, Martín Durán R, Ruano J, Delgado C, et al. Assessment of tricuspid regurgitation by Doppler color flow imaging: angiographic correlation. *Int J Cardiol.* 1994;44(3):275-83.
  55. Haddad F, Doyle R, Murphy DJ, Hunt SA. Right ventricular function in cardiovascular disease, part II: pathophysiology, clinical importance, and management of right ventricular failure. *Circulation.* 2008;117(13):1717-31.



